Supporting information

Co-doped MnS/NiS/Ni_3S_2 in situ grown on hydrophilic nickel foam for energy-efficient urea-assisted alkaline hydrogen production

Haojie Ma[a,b], Muzaffar Ahmad Boda[a], Yang Zhou[a], Chenhao Shi[a], Zhiguo Yi[a,*]

[a]*State Key Lab of High Performance Ceramics and Superfine Microstructure, Shanghai Institute of Ceramics, Chinese Academy of Sciences, Shanghai 201899, China*

[b]*School of Materials Science and Engineering, Materials Genome Institute, Shanghai University, Shanghai 200444, China*

*Corresponding authors

E-mail address: zhiguo@mail.sic.ac.cn

Experimental Section

1. Characterizations

X-ray diffraction (XRD) patterns were collected using X-ray diffractometer (Bruker D8 Advance, Cu Ka radiation λ=0.15404 nm). The morphological, microstructural and elemental mapping were analyzed by field-emission scanning electron microscopy (FESEM, ZEISS Gemini 300), coupled with energy dispersive spectrometry (EDS), and transmission electron microscopy (TEM, FEI Titan G2 60-300) coupled with energy-dispersive X-ray spectroscopy (EDX). Surface elemental composition and valence state were analyzed by X-ray photoelectron spectroscopy (XPS, Thermo fisher Scientific K-Alpha+, with Al Ka radiation of 1486.6 eV). The binding energies were calibrated by setting that of C 1s as 284.8 eV, and the corresponding spectra were fitted by the Thermo Avantage software.

2. Electrochemical Measurements

Electrochemical measurements were carried in a standard three-electrode cell on a Zennium-XC electrochemical workstation, and the chronopotentiometry measurement data was recorded by the CORRRTEST CS310 electrochemical workstation. The prepared catalyst was used as the working electrode, graphite rod as counter electrode and Hg/HgO electrode as reference electrode, and a mixed solution of 1.0 M KOH and 0.33 M urea was used as electrolyte. Prior to electrochemical testing, cyclic voltammetry (CV) test carried at 50 mV s^{-1} was performed for 40 cycles to activate the sample. Linear sweep voltammetry curve (LSV) was recorded at the scanning rate of 5 mV s^{-1} and corrected by IR compensation. The electrochemical impedance spectroscopy (EIS) measurements were conducted over a frequency range of 100 kHz to100 mHz with AC signal amplitude of 5 mV, at an overpotential of -16 mV and 1.3V for the HER and UOR, respectively. Tafel slope based on the LSV curve, was calculated through mapping overpotential and current density (Log| j (mA cm^{-2}) |). The electrochemical active surface area (ECSA) was evaluated by measuring the electrochemical double layer capacitance (C_{dl}) of different samples. For all catalysts,

C_{dl} were obtained from CV tests, carried at the scan rates of 10 mV s^{-1} to 50 mV s^{-1} (10, 20, 30, 40 and 50 mV s^{-1}). The value of C_{dl} was obtained by plotting the difference in charge-discharge current density ($\triangle$J=Ja-Jc). Catalytic stability was evaluated by chrono potentiometry. All electrochemical tests were performed at room temperature and all potentials were calibrated with respect to reversible hydrogen electrode (RHE) under the equation E(RHE)=E(Hg/HgO) +0.098+0.059*pH. The overpotential (η) was calculated according to equation: $\eta = |E_{vs.\ RHE} - 1.23\ V|$.

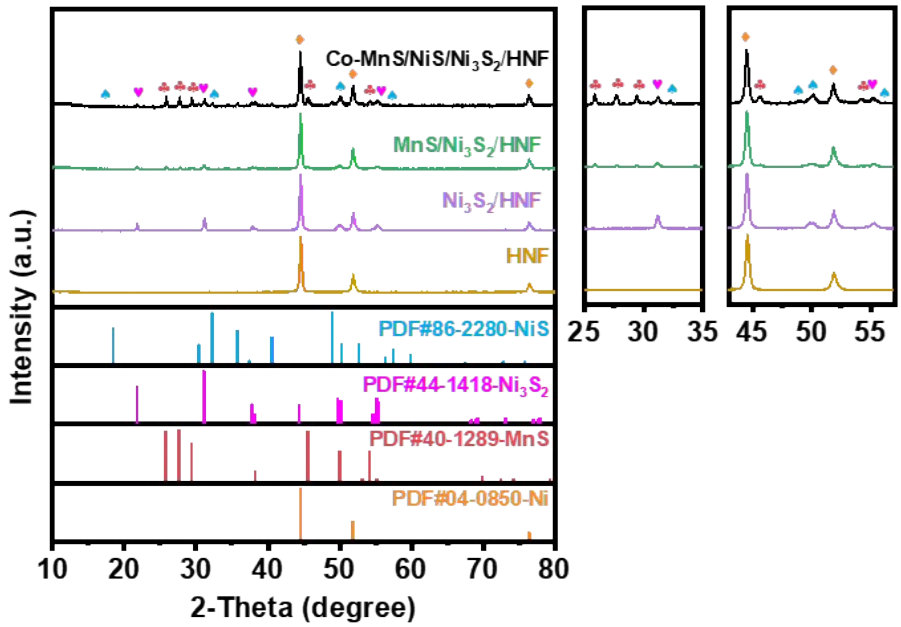

Fig.S1. XRD patterns of the Co-MnS/NiS/Ni_3S_2/HNF, MnS/Ni_3S_2/HNF, Ni_3S_2/HNF and HNF.

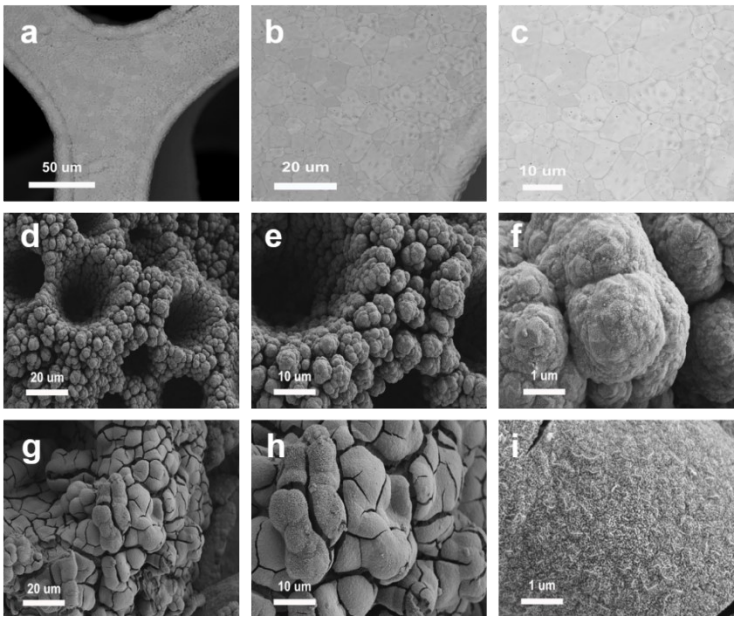

Fig.S2. SEM images of the NF (a-c), HNF (d-f) and Co-MnO_2/$NiMnO_3$/HNF (g-i).

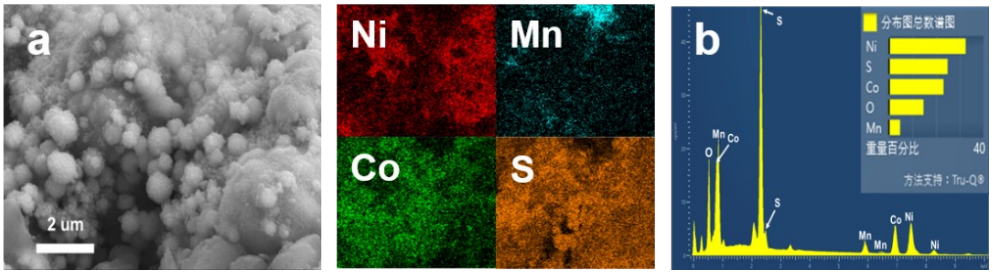

Fig.S3. The elemental mapping spectrums (a) and the corresponding EDX spectrum (b) of the Co-MnS/NiS/Ni_3S_2/HNF catalyst.

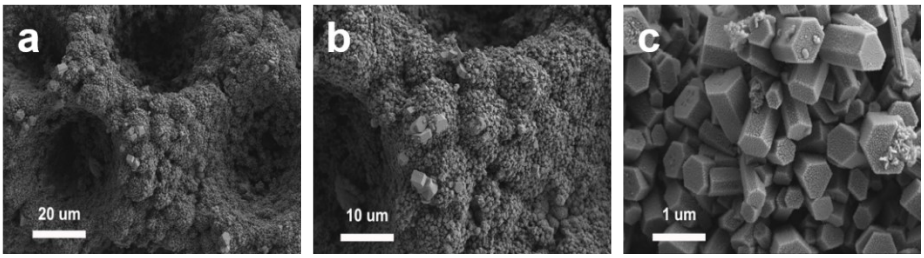

Fig.S4. SEM images (a-c) of the $MnS/Ni_3S_2/HNF$ at different scales.

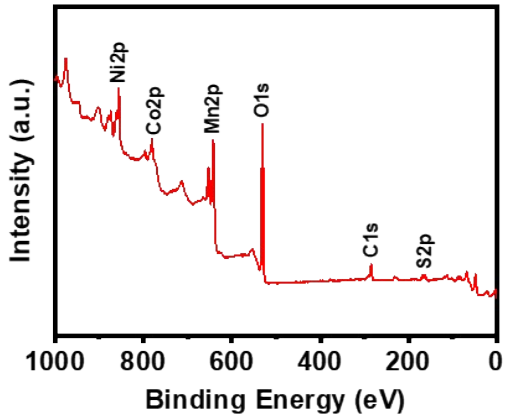

Fig.S5. XPS survey spectrum of $Co\text{-}MnS/NiS/Ni_3S_2/HNF$.

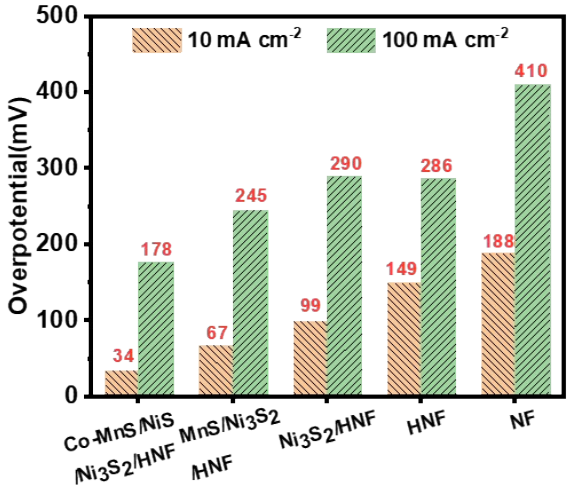

Fig.S6. HER overpotential at different current densities of $Co\text{-}MnS/NiS/Ni_3S_2/HNF$, $MnS/Ni_3S_2/HNF$, Ni_3S_2/HNF, HNF and NF.

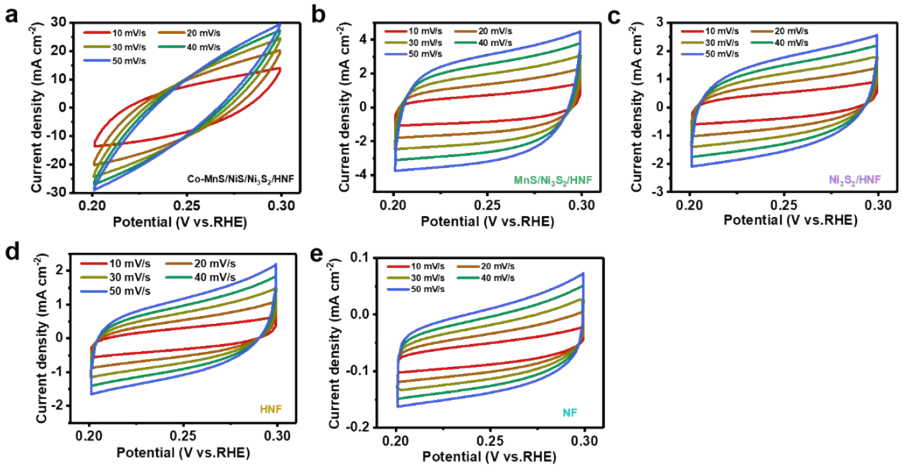

Fig. S8. CV curves of (a) Co-MnS/NiS/Ni_3S_2/HNF, (b) MnS/Ni_3S_2/HNF, (c) Ni_3S_2/HNF, (d) HNF and (e) NF at different scan rates for C_{dl} testing at non-faradic reaction potential region for HER.

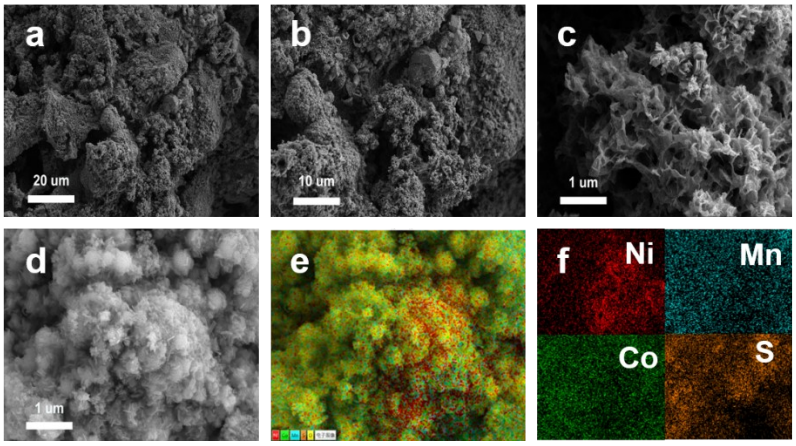

Fig.S9. SEM images (a-c), HAADF image (d), EDS images (e-f) of the Co-MnS/NiS/Ni_3S_2/HNF after HER long-term stability test.

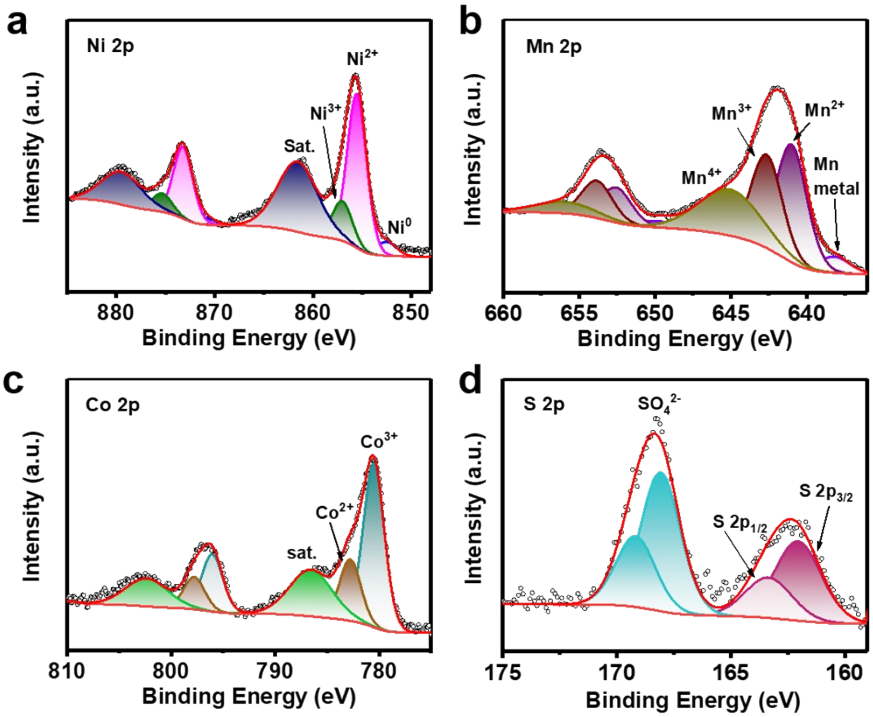

Fig.S9. High-resolution XPS spectrum of Ni 2p (a), Mn 2p (b), Co 2p (c) and S 2p (d) for the Co-MnS/NiS/Ni_3S_2/HNF after HER long-term stability test.

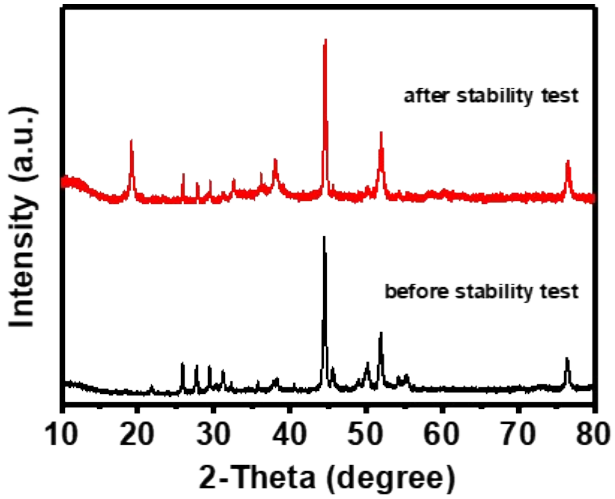

Fig.S10. XRD patterns before and after chronopotentiometry measurement for the Co-MnS/NiS/Ni_3S_2/HNF.

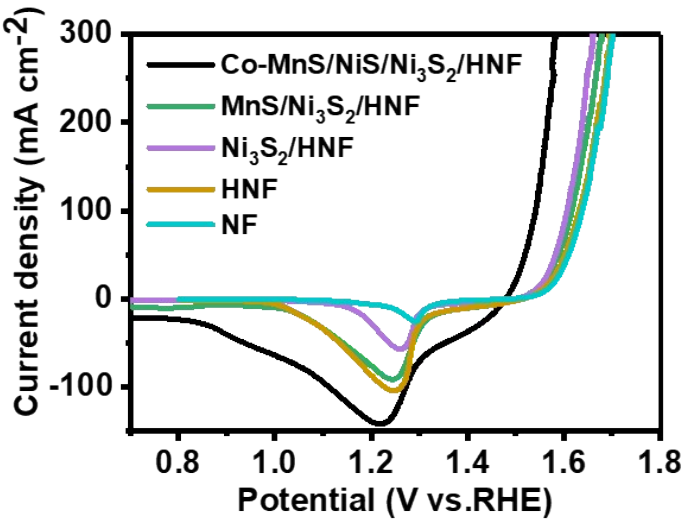

Fig.S11. Polarization curves with iR-compensation of the Co-MnS/NiS/Ni_3S_2/HNF in 1 M KOH.

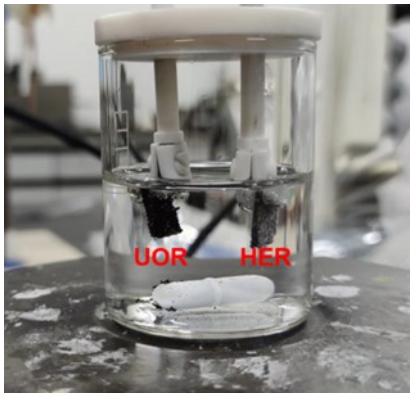

Fig.S12. Photo of urea-assisted hydrogen electrolyzer.

Table.S1. Comparison of the HER performance of Co-MnS/NiS/Ni_3S_2/HNF and other reported non noble metal electrocatalysts.

Catalysts	Voltage (V)@ j(mA cm^{-2})	Stability	Reference
P/Cr60-$NiMoO_4$	35.7 mV @ 10 mA cm^{-2}	100 mA cm^{-2} @ 100 h	[1]
$NiSe_2$/$Ni_{0.85}Se$-2h	76 mV @ 10 mA cm^{-2}	100 mA cm^{-2} @ 100 h	[2]
Ni_3S_2@NiS-250/NF	129 mV @ 10 mA cm^{-2}	250 mV @ 50 h	[3]
NiMoS@NSC	52 mV @ 10 mA cm^{-2}	100 mA cm^{-2} @ 100 h	[4]
N-Ni-MoO_2/NF	49 mV @ 10 mA cm^{-2}	1000 mA cm^{-2} @ 100 h	[5]
Mo-NiS/Ni_3S_2-rich Sv	73 mV @ 10 mA cm^{-2}	30 h	[6]
MoS2 NPs/CoS_2 NTs	99.3 mV @ 10 mA cm^{-2}	50 h	[7]
20% Mn-Ni_3Se_2@NF	217 mV @ 10 mA cm^{-2}	-	[8]
NF-Ni_3S_2/MnO_2	102 mV @ 10 mA cm^{-2}	48 h	[9]
Ni_3S_2@Ni_3P	92 mV @ 10 mA cm^{-2}	-	[10]
CoFeP@Ni_3S_2	50 mV @ 10 mA cm^{-2}	27 h	[11]
Ni_3S_2@MoS_2 CS	98 mV @ 10 mA cm^{-2}	24 h	[12]
N-Co_9S_8/Ni_3S_2/NF	111 mV @ 10 mA cm^{-2}	20 h	[13]
Co-MnS/NiS/Ni_3S_2/HNF	**34 mV @ 10 mA cm^{-2}**	**100 mA cm^{-2} @96 h**	**This work**

Table.S2. Comparison of the UOR performance of Co-MnS/NiS/Ni_3S_2/HNF and other reported non noble metal electrocatalysts.

Catalysts	Electrolyte	Voltage (V)@ j(mA cm^{-2})	Stability	Reference
P/Cr60-$NiMoO_4$	1 M KOH +0.33 M urea	1.36 V @ 100 mA cm^{-2}	100 mA cm^{-2}@60 h	1
$NiSe_2$/$Ni_{0.85}Se$-2h	1 M KOH +0.3 M urea	1.32 V @ 10 mA cm^{-2}	100 mA cm^{-2}@60 h	2
$Co_{0.3}$-Ni_3S_2/$Ni3Sn_2S_2$	1 M KOH +0.5 M urea	1.344 V @ 100 mA cm^{-2}	1.34 V @15 h	14
$LaNiO_3$−NiO	1 M KOH +0.5 M urea	1.34 V @ 10 mA cm^{-2}	1.5 V @1 h	15
N-Ni-MoO_2/NF	1 M KOH +0.5 M urea	1.351 V @ 10 mA cm^{-2}	1000 mA cm^{-2}@100 h	5
MoS_2 NPs/CoS_2 NTs	1 M KOH +0.5 M urea	1.31 V @ 10 mA cm^{-2}	50 h	7
Mo-NiS/Ni_3S_2-rich Sv	1 M KOH +0.5 M urea	1.4 V @ 10 mA cm^{-2}	30 h	6
20% Mn-Ni_3Se_2@NF	1 M KOH +0.33 M urea	1.369 V @ 10 mA cm^{-2}	-	8
Ni_3S_2@Ni_3P	1 M KOH +0.33 M urea	1.36 V @ 10 mA cm^{-2}	12 h	10
CoFeP@Ni_3S_2	1 M KOH +0.5 M urea	1.358 V @ 10 mA cm^{-2}	25 h	11
Co_2P-Ni_3S_2/C	1 M KOH +0.5 M urea	1.338 V @ 10 mA cm^{-2}	96 h	16
CoS_2/MoS_2/Ni_3S_2/NF	1 M KOH +0.5 M urea	1.30 V @ 10 mA cm^{-2}	1.43 V @ 100 h	17
Ni_3S_2@MoS_2 CS	1 M KOH +0.5 M urea	1.336 V @ 10 mA cm^{-2}	24 h	12
N-Co_9S_8/Ni_3S_2/NF	1 M KOH +0.5 M urea	1.37 V @ 100 mA cm^{-2}	20 h	13
Ni_xS_y/NF-3	1 M KOH +0.33 M urea	1.343 V @ 100 mA cm^{-2}	20 h	18
Co-MnS/NiS/Ni_3S_2/HNF	**1 M KOH +0.33 M urea**	**1.313 V @ 50 mA cm^{-2} 1.343 V @ 100 mA cm^{-2}**	**100 mA cm^{-2} @96 h**	**This work**

Notes and references

1 Y. Li, H. Guo, Y. Zhang and R. Song, *Appl. Catal. B-Environ.*, 2024, **341**, 123296.

2 K. Wu, C. Lyu, J. Cheng, Z. Guo, H. Li, X. Zhu, W.-M. Lau and J. Zheng, *Small*, 2023, **20**, 04390.

3 M. Chen, Q. Su, N. Kitiphatpiboon, J. Zhang, C. Feng, S. Li, Q. Zhao, A. Abudula, Y. Ma and G. Guan, *Fuel*, 2023, **331**, 125794.

4 X. Fan, B. Li, C. Zhu, F. Yan, X. Zhang and Y. Chen, *Small*, 2024, 2309655.

5 G. Qian, T. Lu, Y. Wang, H. Xu, X. Cao, Z. Xie, C. Chen and D. Min, *Chem. Eng. J.*, 2024, **480**, 147993.

6 K. Zhang, Y. Duan, N. Graham and W. Yu, *Appl. Catal. B-Environ.*, 2023, **323**, 122144.

7 T. L. L. Doan, D. C. Nguyen, K. Kang, A. Ponnusamy, H. I. Eya, N. Y. Dzade, C. S. Kim and C. H. Park, *Appl. Catal. B-Environ.*, 2024, **342**, 123295.

8 A. M. Shah, K. H. Modi, P. M. Pataniya, K. S. Joseph, S. Dabhi, G. R. Bhadu and C. K. Sumesh, *ACS Appl. Mater. Interfaces*, 2024, **16**, 11440–11452.

9 Y. Xiong, L. Xu, C. Jin and Q. Sun, *Appl. Catal. B-Environ.*, 2019, **254**, 329-338.

10 X. Guo, L. Qiu, M. Li, F. Tian, X. Ren, S. Jie, S. Geng, G. Han, Y. Huang, Y. Song, W. Yang and Y. Yu, *Chem. Eng. J.*, 2024, **483**, 149264.

11 W. Peng, D. Wen, W. Zhang, W. Li, Y. Lu, D. Zhou and W. Hu, *Appl. Surf. Sci.*, 2024, **642**, 158599.

12 Q. Li, B. Yuan, B. Zhang, Y. Ji, H. Xie, Y. Xie, Y. Dong, Z. Liu, Y. Liu, L. Qiao, R. Ke, C. Yang, J. Han and W. He, *J. Electroanalytical. Chem.*, 2023, **931**, 117185.

13 H. Xie, Y. Feng, X. He, Y. Zhu, Z. Li, H. Liu, S. Zeng, Q. Qian and G. Zhang, *Small*, 2023, 2207425.

14 H. Zhao, M. Liu, X. Du and X. Zhang, *Int. J. Hydrogen Energy*, 2024, **58**, 117-127.

15 H. Ding, Z. Zhao, H. Zeng, X. Li, K. Cui, Y. Zhang and X. Chang, *ACS Mater. Lett.*, 2024, **6**, 1029-1041.

16 T. Chen, Q. Wu, F. Li, R. Zhong and Z. Chen, *ACS Appl. Nano Mater.*, 2023, **6**, 18364-18371.

17 Y. Zhang, H. Guo, M. Song, Z. Qiu, S. Wang and L. Sun, *Appl. Surf. Sci.*, 2023, **617**, 156621.

18 H. Liu, D. Wen and B. Zhu, *J. Electroanal. Chem.*, 2023, **928**, 117082.